VIP Bioinorganic Chemistry

DOI: 10.1002/ange.201300861

A High-Valent Heterobimetallic $[Cu^{III}(\mu\text{-}O)_2Ni^{III}]^{2+}$ Core with Nucleophilic Oxo Groups**

Subrata Kundu, Florian Felix Pfaff, Enrico Miceli, Ivelina Zaharieva, Christian Herwig, Shenglai Yao, Erik R. Farquhar, Uwe Kuhlmann, Eckhard Bill, Peter Hildebrandt, Holger Dau, Matthias Driess, Christian Limberg,* and Kallol Ray**

The study of heterobimetallic dioxygen complexes is interesting with regard to their potential in modeling the structures and reactivities of metalloenzymes containing two different metal ions at their active sites.[1] Moreover, such investigations may lead to the discovery of novel species exhibiting alternative reactivity patterns with respect to their symmetric counterparts. However, in contrast to the numerous reports of biomimetic synthetic dinuclear complexes involving homometallic dioxygen cores,[2] reports on mixed-metal $[MO_2M']^{n+}$ cores are relatively rare,[3] presumably because of intrinsic challenges associated with their preparation by the methods usually used to obtain their symmetric analogues. A limited number of heterobimetallic dioxygen complexes has been made in the past, either by the reaction of heterobimetallic M–M′ precursors with dioxygen, or by reaction of a well-defined metal–dioxygen subunit with a reducing heterometal complex.[3a] The latter strategy has also been used recently by some of us[3d] to synthesize and structurally characterize the first example of a heterodinuclear peroxo complex, {Ni(μ-O_2)K}, by a one-electron reduction of a room-temperature stable nickel superoxo complex $[LNi^{II}(O_2)]$ (**1**; L = [HC-$(CMeNC_6H_3(i\text{Pr})_2)_2$])[4] with elemental potassium. Furthermore, replacement of the potassium ion in the $[Ni(\mu\text{-}O_2)K]^{n+}$ core by Zn^{2+} or Fe^{+} ions initiated peroxido O–O bond scission and subsequent H-atom abstraction to generate the heterobimetallic bis(μ-hydroxo) Ni–Zn[3d] or alkoxo hydroxido Ni–Fe[3e] complexes, respectively. Theoretical studies[3d,e] suggested the involvement of heterobimetallic $Ni(\mu\text{-}O)_2M'$ (M′ = Zn, Fe) cores in the H-atom abstraction process; their electronic structures and reactivities were predicted to be strongly dependent on the nature of the second metal ion. Unfortunately, these intermediates could not be directly detected by spectroscopic methods and hence the predictions of the theoretical calculations could not be verified experimentally .

We now demonstrate the low-temperature trapping of the proposed heterobimetallic bis(μ-oxo) intermediate during the one-electron reduction of **1** using a Cu^{I} triamine complex, $[Cu(MeAN)](BF_4)$ [**2**-BF_4; MeAN=*N*,*N*,*N*′,*N*′,*N*″-pentamethyl dipropylenetriamine],[5] as a reductant. We report the synthesis of the $[LNi^{III}(\mu\text{-}O)_2Cu^{III}(MeAN)]^{+}$ complex **3** (Scheme 1), in nearly quantitative yield, and its characterization with optical, electron paramagnetic resonance (EPR), resonance Raman (rRaman), and X-ray absorption spectroscopies (XAS), as well as electrospray ionization mass spectrometry (ESI-MS), reactivity studies, and density functional theory (DFT) calculations. Interestingly, the oxo groups of **3** act as nucleophiles, in sharp contrast to the electrophilic oxo groups of the well characterized homometallic $[Ni_2(\mu\text{-}O)_2]^{2+}$ and $[Cu_2(\mu\text{-}O)_2]^{2+}$ analogues. In fact, complex **3** represents the only example of a high-valent[6] bis(μ-oxo)dimetal core involving nucleophilic oxo groups that can perform deformylation of aldehydes. Until this report, only metal-bound peroxides[7] were believed to be sufficiently nucleophilic to attack aldehydes leading to production of formate and oxidized coproducts. This study, therefore, underlines the importance of subtle electronic changes in the reactivity of the biologically relevant metal–dioxygen intermediates.

[*] S. Kundu, F. F. Pfaff, E. Miceli, Dr. C. Herwig, Prof. Dr. C. Limberg, Dr. K. Ray
Humboldt-Universität zu Berlin, Institut für Chemie
Brook-Taylor-Strasse 2, 12489 Berlin (Germany)
E-mail: christian.limberg@chemie.hu-berlin.de
kallol.ray@chemie.hu-berlin.de

Dr. I. Zaharieva, Prof. Dr. H. Dau
Freie Universität Berlin, FB Physik, Berlin (Germany)

Dr. S. Yao, Dr. U. Kuhlmann, Prof. Dr. P. Hildebrandt, Prof. Dr. M. Driess
Technische-Universität Berlin, Institut für Chemie
Strasse des 17 Juni 135, 10623 Berlin (Germany)
E-mail: matthias.driess@tu-berlin.de

Dr. E. R. Farquhar
Case Western Reserve University Center for Synchrotron Biosciences and Center for Proteomics and Bioinformatics, Brookhaven National Laboratory (USA)

Dr. E. Bill
Max-Plank-Institut für chemische Energiekonversion, Mülheim an der Ruhr (Germany)

[**] We gratefully acknowledge financial support of this work from the Cluster of Excellence "Unifying Concepts in Catalysis" (EXC 314/1), Berlin. XAS data were obtained on beamline X3B of the National Synchrotron Light Source (Brookhaven National Laboratory) and beamline KMC-1 of BESSY, Berlin (Germany). Beamline X3B is operated by the Case Western Reserve University Center for Synchrotron Biosciences, supported by NIH Grant P30-EB-009998. NSLS is supported by the United States Department of Energy, Office of Science, Office of Basic Energy Sciences, under Contract DE-AC02-98CH10886. We also thank Prof. William B. Tolman for helpful suggestions.

Supporting information for this article is available on the WWW under http://dx.doi.org/10.1002/anie.201300861.

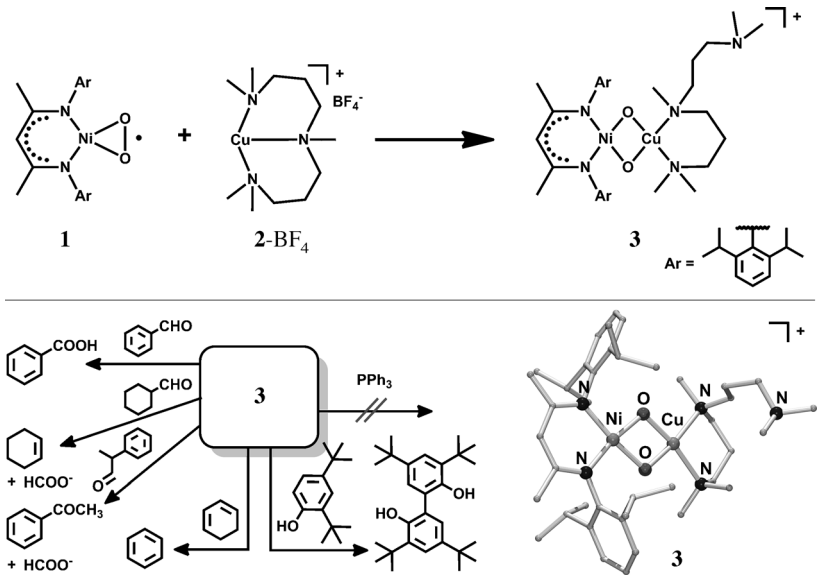

Scheme 1. Formation, DFT calculated structure, and products of the reactions of **3** with different substrates.

Combination of equimolar amounts of **1** and **2**-BF_4 at −90 °C in CH_2Cl_2 leads to the immediate generation of a metastable intermediate **3** ($t_{1/2}$ = 900 s at −50 °C) with absorption maxima λ_{max} (ε_{max}; $M^{-1}cm^{-1}$) centered at 300 (20000), 370 (13500), and 895 (5000) nm (Figure 1). The electrospray mass spectrum (Supporting Information Figure S1) of **3** exhibits the most prominent peak at a mass–charge ratio (*m*/*z*) of 771.38, with a mass and isotope distribution pattern corresponding to $[LNi(O)_2Cu(MeAN)]^+$. When the reaction is carried out with ^{18}O enriched **1**, a mass peak corresponding to $[LNi(^{18}O)_2Cu(MeAN)]^+$ appears at *m*/*z* 775.38, thereby revealing the presence of two oxygen atoms in **3**. Although, we are currently unable to assign the low-energy band in the absorption spectrum of **3**, the similarity of the features at λ_{max} = 300–400 nm to ones typical of homometallic $[Ni_2(\mu\text{-}O)_2]^{2+}$ and $[Cu_2(\mu\text{-}O)_2]^{2+}$ cores[2] may suggest an analogous formation of a bis μ-oxo core in **3**. Indeed, the rRaman (Figure 1) spectrum of **3** using 413 nm laser excitation in resonance with the 370 nm transition supports the view of a $[Ni(\mu\text{-}O)_2Cu]^{2+}$ structure. The band at 625 cm^{-1} of **3** [ν(**3**-^{16}**O**^{16}**O**)] shifts down to 595 cm^{-1} [ν(**3**-^{18}**O**^{18}**O**)] in the corresponding $^{18}O_2$-substituted complex **3**. Furthermore, single oxygen-isotope labeling experiments[8] show an additional intermediate band at 615 cm^{-1} corresponding to the vibration of the partially labeled species [ν(**3**-^{16}**O**^{18}**O**)]. In analogy to the well-studied $[M_2(\mu\text{-}O)_2]^{2+}$ (M = Fe, Ni, Cu) systems, for which similar rRaman signatures and oxygen isotope effects were reported,[9] we assign the rRaman feature at 625 cm^{-1} to a tetra-atomic vibration (Figure S2) mode of the $[Ni(\mu\text{-}O)_2Cu]^{2+}$ core. This assignment is also supported by DFT calculations (see below). Furthermore, the fact that the frequency of ν(**3**-^{16}**O**^{18}**O**) is not halfway between ν(**3**-^{16}**O**^{16}**O**) and ν(**3**-^{18}**O**^{18}**O**), and the lack of isotope-sensitive bands in the 700–1200 cm^{-1} range, strongly argue against the presence of any peroxo or superoxo species.

X-ray absorption spectroscopic studies were performed at Cu and Ni K-edges to directly probe the metal oxidation states in **3**. Figure 2 A shows a comparison of the Cu K-edge spectrum of **3** with the spectra of its Cu^I precursor and the previously reported [(AN)Cu^{II}(NHTs)] [**4**, AN = 3,3′-iminobis(*N*,*N*-dimethyl propylamine; Ts = tosyl][10] complex. A progressive blue shift in the edge energy from **2**-BF_4 to **4** to **3** is in accord with a stepwise increase in the oxidation state of copper in the series. Most importantly, a 2 eV blueshift, from 8978 to 8980 eV, and a broadening of the pre-edge are observed from **4** to **3**, which strongly suggest[11] the presence of a Cu^{III} ion in **3**. In addition, the Ni K-edge data (Figure 2 B), which display a subtle blueshift and reduced intensity for the pre-edge, as well as a broader blueshift of the overall edge in **3** relative to its nickel(II) superoxide precursor, are consistent with a nickel-based oxidation from **1** to

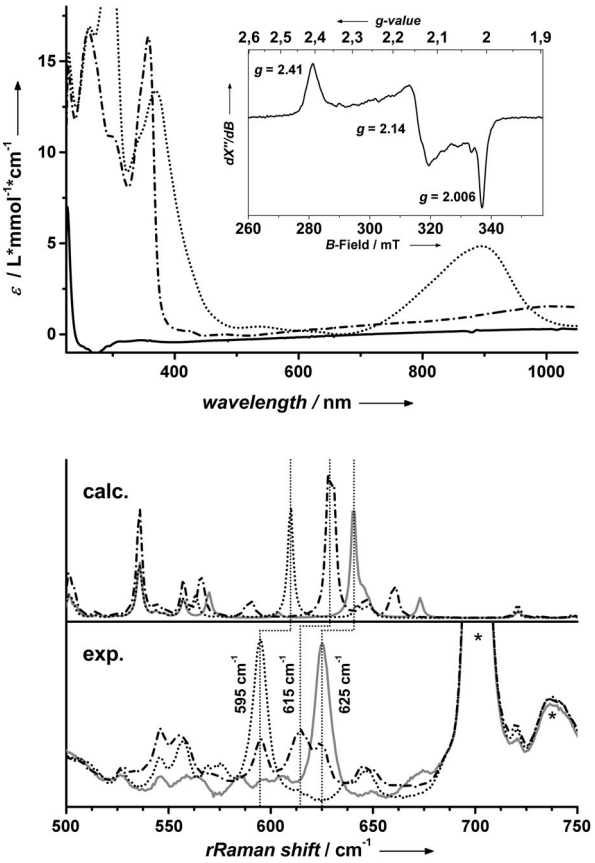

Figure 1. Top: Absorption spectra of **2**-BF_4 (solid trace), **1** (dash–dot trace), **3** (dotted trace) in CH_2Cl_2 at −90 °C. Inset: X-band EPR spectrum of **3** in CH_2Cl_2 (0.47 mM) at 10 K (frequency 9.470251 GHz; power 0.05 mW; modulation 0.5 mT). Bottom: Calculated (DFT, see Supporting Information for details) and experimental (CH_2Cl_2; −90 °C; 413 nm excitation) rRaman spectra of **3**-$^{16}O_2$ (gray, solid trace), **3**-$^{18}O_2$ (dotted trace), and **3**-^{16}**O**^{18}**O** (dash–dot trace). Bands originating from the solvent are marked by asterisks.

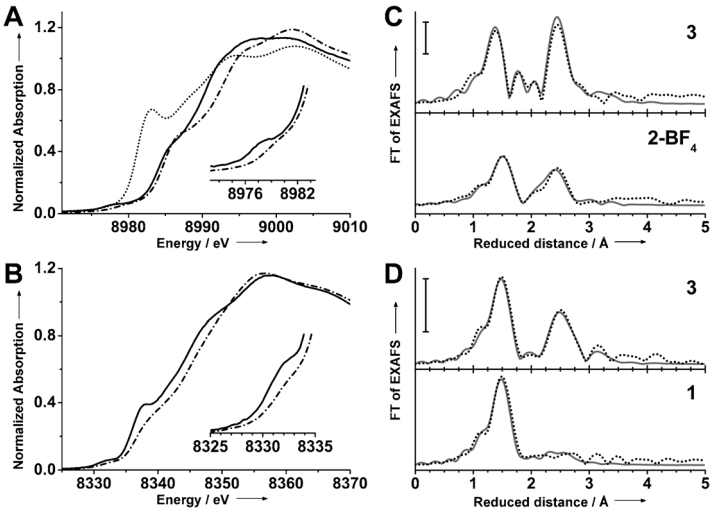

Figure 2. A) Normalized Cu K-edge XANES spectra for **2**-BF_4 (dotted line), **3** (dash–dot line), and **4** (solid line). The inset depicts an expansion of the pre-edge region for **3** and **4**. B) Normalized Ni K-edge XANES spectra for **1** (solid line) and **3** (dash–dot line). The inset shows an expansion of the pre-edge region. C) Fourier-transformed Cu K-edge EXAFS spectra of **2**-BF_4 and **3** (Experiment: dotted line; simulation: bold line). D) Fourier-transformed Ni K-edge EXAFS spectra of **1** and **3**. For the EXAFS data on a wavevector scale before calculation of the Fourier transform see Figure S3.

3.[12] The X-band EPR spectrum (Figure 1) of **3** is also found to be in good agreement with the $[LNi^{III}(\mu\text{-}O)_2Cu^{III}(MeAN)]^+$ assignment and is dominated by a typical $S = 1/2$ Ni^{III} rhombic signal ($g_x = 2.006$, $g_y = 2.14$, $g_z = 2.41$) that lacks the hyperfine splitting characteristic of Cu^{II},[13] and corresponds, by integration, to 90% of the amount of **2**-BF_4 added. The absence of hyperfine splitting indicates copper in the diamagnetic $3d^8$ low-spin state, which moreover reveals planar coordination.

Extended X-ray absorption fine structure (EXAFS) analysis reveals further structural details (Figure 2C; Figure 2D and S3; Table S1). For **1** a shell of four N/O scatterers at 1.84 Å is obtained from Ni EXAFS, in good agreement with the molecular structure determined previously by X-ray crystallography (Table S2).[4] On the other hand, a fit to the data for **3** requires two subshells of N/O scatterers at 1.79 Å (assigned to the two Ni^{III}–O units) and 1.88 Å (assigned to the two Ni^{III}–N units), consistent with the structure derived from DFT calculations (Table S2). In addition, Ni EXAFS of **3** shows an additional peak at 2.81 Å corresponding to the Cu scatterer, thereby strongly supporting the presence of a heterodinuclear Ni···Cu center in **3**. Further support for including a Ni···Cu distance at 2.81 Å comes from Cu EXAFS, which also detects the Ni scatterer at 2.81 Å in **3**, but not in the mononuclear Cu^I precursor. Furthermore, the best fit of the Cu EXAFS of **3** can be obtained with two subshells, each containing two O/N scatterers at 1.80 Å and 2.00 Å, thereby supporting a four coordinate Cu center in **3**. It is important to note that a fit with two O/N scatterers at 1.88 Å and three O/N scatterers at 2.00 Å gave a high Debye–Waller factor, which together with the DFT calculations (see below) preclude the presence of a five-coordinate Cu center in **3** (Table S1).

DFT calculations (see Supporting Information for details) on **3** yield a minimum energy for a C_1 structure (Scheme 1; Figure S4; Table S3) with a four-coordinate planar geometry at both the copper and the nickel centers, and geometrical parameters in excellent agreement with that obtained from XAS studies (Table S2). In the calculated structure MeAN acts as a bidentate ligand, with one of the terminal tertiary amine nitrogen atoms remaining out of the coordination sphere of Cu. The ground state is calculated to be $S = 1/2$, consistent with the EPR studies. The unpaired spin is distributed such that the nickel center has 0.7 spin, whilst the copper and oxygen centers carry an average spin density of only 0.01 and 0.06, respectively (Table S4). These results reveal the presence of Ni^{III} ($S = 1/2$; $3d^7$) and Cu^{III} ($S = 0$; $3d^8$) centers in **3**, thereby, supporting a $[LNi^{III}(\mu\text{-}O)_2Cu^{III}(MeAN)]^+$ assignment. Vibrational analysis on the DFT-optimized structure of **3** in the $S = 1/2$ ground state predicts a strong $[Ni^{III}(\mu\text{-}O)_2Cu^{III}]^{2+}$ core vibrational mode at 640 cm^{-1} (Figures S5–S6; Table S5). This frequency and in particular the calculated $^{18}O/^{16}O$ isotopic shifts are in excellent agreement with the experimental data (Figure 1). Thus, the spectroscopic results validate the calculated molecular and electronic structures of **3**.

The oxo groups in high-valent $[M_2(\mu\text{-}O)_2]^{n+}$ (M = Fe, Co, Ni, Cu) cores act as strong electrophiles and are typically unreactive towards other electrophiles.[2] Consistent with these observations, addition of cyclohexane carboxaldehyde (CCA) or 2-phenylpropionaldehyde (2-PPA) to $[(AN)_2Cu_2(\mu\text{-}O)_2]^{2+}$ [5,14] or $[(L)_2Ni_2(\mu\text{-}O)_2]$,[15] which are the homometallic analogues of **3**, at −90 °C does not change the UV/Vis spectra. In contrast, similar reactions with **3** result in instantaneous bleaching and disappearance of the bands at 370 and 895 nm in the UV/Vis absorption spectrum (Figure S7). Product analysis of the reaction mixture reveals the formation of the deformylated[16] products in 65–90% yields (Scheme 1; Table S6). The reactivity of **3** was further investigated using benzoyl chloride at −50 °C, to confirm the nucleophilic properties of **3**. A pseudo-first order decay of the absorption feature at 895 nm and the subsequent formation of benzoic acid (Figure S8) were observed upon adding benzoyl chloride to a preformed solution of **3** at −50 °C. The rate constant increases proportionally with the substrate concentration, affording a second-order rate constant, k_2, of $0.11\,M^{-1}s^{-1}$ at −50 °C. Additional mechanistic studies with *para*-substituted benzoyl chloride (*para*-Y-C_7H_4OCl; Y = OMe, Me, H, Cl, CN) reveal a good linear correlation of the rate to the σ_P^+ values of the *para* substituents. A positive Hammett ρ value of 2.5 (Figure S9) is obtained, which further supports the nucleophilic character of the $[LNi^{III}(\mu\text{-}O)_2Cu^{III}(MeAN)]^+$ core in the oxidation of benzoyl chloride. To our knowledge, **3** is the only example of a high-valent[6] bis(μ-oxo) dimetal complex containing nucleophilic oxo groups. To investigate in how far the dangling amine group assists reactivity or is even responsible for the observed nucleophilicity, experiments with *N,N,N′,N′*-tetramethylethylenediamine (TMEDA), as a co-ligand for Cu instead of MeAN were envisaged. Unfortunately, unlike **2**-BF_4, the Cu^I(TMEDA) complex has been reported to be unstable,[17] so that it had to be generated in situ prior to the reaction with **1**.

Preliminary experiments with the resulting complex $[LNi^{III}(\mu\text{-}O)_2Cu^{III}(TMEDA)]^+$ (**5**, Scheme S1),[18] structurally similar to **3**, but lacking any dangling amine group, suggest that the dangling amine group may not be the origin of the nucleophilic behavior of the oxido ligands within **3**: complex **5** reacts with benzoyl chloride at −90 °C in acetone at a rate much faster than **3** (Figure S12). However, the possibility that the nucleophilic reactivity is actually initiated by the slight excess of TMEDA present in the solution because of incomplete complexation cannot be excluded at this point. In this context it is also worth mentioning that $[(AN)_2Cu_2(\mu\text{-}O)_2]^{2+}$ may also be expected to have dangling or at least loose amine arms and is an electrophilic oxidant.

Complex **3** also performs hydrogen atom abstraction from the C–H (or O–H) bonds of 1,3-cyclohexadiene (CHD), 9,10-dihydroanthracene (DHA), 2,4-di-*tert*-butylphenol (2,4-DTBP), and 2,6-di-*tert*-butylphenol (2,6-DTBP); the second-order rate constants derived from these studies in CH_2Cl_2 solution are listed in Table S6. Surprisingly, the rates for reactions with DHA and 2,6-DTBP are found to be significantly lower than those determined for CHD and 2,4-DTBP, respectively. Since DHA/CHD and 2,4-DTBP/2,6-DTBP have comparable C–H and O–H bond dissociation energies,[19] the large rate differences observed for **3** suggest that the β-diketiminate ligand impedes access of the bulkier DHA or 2,6-DTBP to the $[LNi^{III}(\mu\text{-}O)_2Cu^{III}(MeAN)]^+$ core. Such sterically derived mitigation of reactivity has been observed for other β-diketiminate-ligated systems.[20] No reaction of **3** with triphenyl phosphine has been observed.

A number of enzymes[21,22] use a bimetallic active site to bind and activate dioxygen to form reactive species involving superoxide, peroxide, and metal oxide cores, which are then responsible for carrying out a variety of electrophilic and nucleophilic oxidation reactions. While nucleophilic reactions are typically carried out by superoxides or peroxides, electrophilic reactions are attributed to metal oxides. For example, the $[Cu_2(\mu\text{-}O)_2]^{2+}$ and $[Fe_2(\mu\text{-}O)_2]^{4+}$ cores have been considered as active oxidants in the hydroxylation of phenol and methane by tyrosinase and soluble methane monooxygenase, respectively.[2,21] On the other hand, a homo- or heterodinuclear peroxo core[22] has been proposed as the active species responsible for the deformylation of fatty aldehydes by cyanobacterial aldehyde decarbonylase (AD); the metal centers in the dimetal-cofactor of AD have yet to be identified. In this work, we have now reported the synthesis and spectroscopic characterization of a high-valent heterodinuclear $[Ni^{III}(\mu\text{-}O)_2Cu^{III}]^{2+}$ core, which can act as nucleophile to attack (among other electrophiles) aldehydes leading to production of formate and oxidized coproducts. The nucleophilic property of **3**, which is in sharp contrast to the electrophilicity of oxo groups in the homodinuclear analogues containing $[Cu_2(\mu\text{-}O)_2]^{2+}$ or $[Ni_2(\mu\text{-}O)_2]^{2+}$ cores, may be related to a reduced covalency of the metal–oxygen bonds owing to the mismatch of the bonding orbitals in the asymmetric $[Ni^{III}(\mu\text{-}O)_2Cu^{III}]^{2+}$ core. Further experimental and theoretical studies are, however, warranted to understand the origin of the nucleophilic behavior of **3**. These studies are ongoing.

In conclusion, we have reported the synthesis and spectroscopic characterization of the mixed-metal Ni–Cu bis (μ-oxo) complex **3** that is potent in the deformylation of aldehydes. Whether or not a similar asymmetric bis(μ-oxo) core also acts as an active species in the catalytic cycle of cyanobacterial AD is now a particularly intriguing question.

Received: January 31, 2013
Published online: April 15, 2013

Keywords: bridging oxo ligands · copper · diamond core · nickel · nucleophilicity

[1] a) V. R. I. Kaila, M. I. Verkhovsky, M. Wikström, *Chem. Rev.* **2010**, *110*, 7062; b) J. P. Klinman, *Chem. Rev.* **1996**, *96*, 2541; c) J. A. Tainer, E. D. Getzoff, K. M. Beem, J. S. Richardson, D. C. Richardson, *J. Mol. Biol.* **1982**, *160*, 181; d) Y. Matoba, T. Kumagai, A. Yamamoto, H. Yoshitsu, M. Sugiyama, *J. Biol. Chem.* **2006**, *281*, 8981.

[2] a) J. Hohenberger, K. Ray, K. Meyer, *Nat. Commun.* **2012**, *3*, 720, DOI: 10.1038/ncomms1718; b) S. Fukuzumi, K. D. Karlin, *Coord. Chem. Rev.* **2013**, *257*, 187; c) E. A. Lewis, W. B. Tolman, *Chem. Rev.* **2004**, *104*, 1047; d) L. M. Mirica, X. Ottenwaelder, T. D. P. Stack, *Chem. Rev.* **2004**, *104*, 1013; e) M. T. Kieber-Emmons, C. G. Riordan, *Acc. Chem. Res.* **2007**, *40*, 618; f) S. Friedle, E. Reisner, S. J. Lippard, *Chem. Soc. Rev.* **2010**, *39*, 2768.

[3] a) I. Garcia-Bosch, X. Ribas, M. Costas, *Eur. J. Inorg. Chem.* **2012**, 179; b) N. W. Aboelella, J. T. York, A. M. Reynolds, K. Fujita, C. R. Kinsinger, C. J. Cramer, C. G. Riordan, W. B. Tolman, *Chem. Commun.* **2004**, 1716; c) J. T. York, A. Llobet, C. J. Cramer, W. B. Tolman, *J. Am. Chem. Soc.* **2007**, *129*, 7990; d) S. Yao, Y. Xiong, M. Vogt, H. Grutzmacher, C. Herwig, C. Limberg, M. Driess, *Angew. Chem.* **2009**, *121*, 8251; *Angew. Chem. Int. Ed.* **2009**, *48*, 8107; e) S. Yao, C. Herwig, Y. Xiong, A. Company, E. Bill, C. Limberg, M. Driess, *Angew. Chem.* **2010**, *122*, 7208; *Angew. Chem. Int. Ed.* **2010**, *49*, 7054.

[4] S. Yao, E. Bill, C. Milsmann, K. Wieghardt, M. Driess, *Angew. Chem.* **2008**, *120*, 7218; *Angew. Chem. Int. Ed.* **2008**, *47*, 7110.

[5] H.-C. Liang, C. X. Zhang, M. J. Henson, R. D. Sommer, K. R. Hatwell, S. Kaderli, A. D. Zuberbühler, A. L. Rheingold, E. I. Solomon, K. D. Karlin, *J. Am. Chem. Soc.* **2002**, *124*, 4170.

[6] Low-valent homodinuclear Pd^{II} or Pt^{II} bis(μ-oxo)cores are, however, known with nucleophilic oxo groups; the oxo basicity arises from strong repulsion between electron-rich oxo groups and Pd^{II} or Pt^{II} centers (W. Li, C. L. Barnes, P. R. Sharp, *J. Chem. Soc. Chem. Commun.* **1990**, 1634; and Ref. [3c]).

[7] a) D. D. LeCloux, A. M. Barrios, S. J. Lippard, *Bioorg. Med. Chem.* **1999**, *7*, 763; b) D. L. Wertz, J. S. Valentine, *Metal-Oxo and Metal-Peroxo Species in Catalytic Oxidations*, *Vol. 97*, Springer, Berlin, **2000**, p. 37; c) J. Cho, S. Jeon, S. A. Wilson, L. V. Liu, E. A. Kang, J. J. Braymer, M. H. Lim, B. Hedman, K. O. Hodgson, J. S. Valentine, E. I. Solomon, W. Nam, *Nature* **2011**, *478*, 502; d) J. Cho, R. Sarangi, J. Annaraj, S. Y. Kim, M. Kubo, T. Ogura, E. I. Solomon, W. Nam, *Nat. Chem.* **2009**, *1*, 568; e) J. Cho, R. Sarangi, W. Nam, *Acc. Chem. Res.* **2012**, *45*, 1321.

[8] Using $^{16/18}O_2$ (a statistical mixture of $^{16}O_2$, $^{16}O^{18}O$, and $^{18}O_2$ in 1:2:1 ratio) complex **1** was formed, which was then treated with **2**-BF_4 to form **3** for rRaman measurements.

[9] a) P. L. Holland, C. J. Cramer, E. C. Wilkinson, S. Mahapatra, K. R. Rodgers, S. Itoh, M. Taki, S. Fukuzumi, L. Que, Jr., W. B. Tolman, *J. Am. Chem. Soc.* **2000**, *122*, 792; b) E. C. Wilkinson, Y. Dong, Y. Zang, H. Fujii, R. Fraczkiewicz, G. Fraczkiewicz, R. S. Czernuszewicz, L. Que, Jr., *J. Am. Chem. Soc.* **1998**, *120*, 955.

[10] S. Kundu, E. Miceli, E. Farquhar, F. F. Pfaff, U. Kuhlmann, P. Hildebrandt, B. Braun, C. Greco, K. Ray, *J. Am. Chem. Soc.* **2012**, *134*, 14710.
[11] J. L. DuBois, P. Mukherjee, T. D. P. Stack, B. Hedman, E. I. Solomon, K. O. Hodgson, *J. Am. Chem. Soc.* **2000**, *122*, 5775.
[12] G. J. Colpas, M. J. Maroney, C. Bagyinka, M. Kumar, W. S. Willis, S. L. Suib, N. Baidya, P. K. Mascharak, *Inorg. Chem.* **1991**, *30*, 920.
[13] The wiggles in the EPR spectrum, faintly reminiscent of hyperfine lines, arise from uneven freezing of the sample resulting in microcrystals of defined orientation. This is concluded on the basis of the observed variations upon repeated freezing or rotating the EPR tube (Figure S10). Also labeling **3** with ^{63}Cu did not systematically affect the pattern.
[14] The corresponding $[(MeAN)_2Cu_2(\mu\text{-}O)_2]^{2+}$ complex does not exist (Ref. [5]). Rather a peroxo bridged complex $[(MeAN)_2Cu_2(\mu\text{-}O_2)]^{2+}$ is formed, which is also found to be unreactive towards aldehydes.
[15] $[(L)_2Ni_2(\mu\text{-}O)_2]$ is formed by the reaction of **1** with its Ni^I precursor (S. Pfirrmann, S. Yao, B. Ziemer, R. Stösser, M. Driess, C. Limberg, *Organometallics* **2009**, *28*, 6855) at −90 °C in CH_2Cl_2. Formation of the bis(μ-oxo) core was confirmed on the basis of the appearance of the absorption band at 400 nm, which is common to all $[Ni_2(\mu\text{-}O)_2]$ cores, and also by ESI-MS methods.
[16] Formate is identified by conversion into its 2-nitrophenylhydrazide (2NPH) derivative, whose ESI-MS spectrum exhibits an intense peak at *m*/*z* 180 (Ref. [22]).
[17] P. Kang, E. Bobyr, J. Dustman, K. O. Hodgson, B. Hedman, E. I. Solomon, T. D. P. Stack, *Inorg. Chem.* **2010**, *49*, 11030.
[18] Complex **5** ($t_{1/2} = 1.5$ h at −90 °C) was generated by adding **1** to a precooled (−90 °C) solution of equimolar amounts of $[Cu(MeCN)_4]OTf$ and TMEDA in acetone. The absorption spectrum (Figure S11) of **5** was found to be very similar to that of **3**; this further confirms that the Cu center in **3** is also four coordinate as in **5**. Reactions with benzoyl chloride were performed with 1 mM solutions of **5** in acetone at −90 °C.
[19] Y.-R. Luo, *Comprehensive handbook of chemical bond energies*, Taylor & Francis, New York, **2007**.
[20] N. W. Aboelella, E. A. Lewis, A. M. Reynolds, W. W. Brennesel, C. J. Cramer, W. B. Tolman, *J. Am. Chem. Soc.* **2002**, *124*, 10660.
[21] a) E. I. Solomon, P. Chen, M. Metz, S.-K. Lee, A. E. Palmer, *Angew. Chem.* **2001**, *113*, 4702; *Angew. Chem. Int. Ed.* **2001**, *40*, 4570; b) M. H. Sazinsky, S. J. Lippard, *Acc. Chem. Res.* **2006**, *39*, 558.
[22] N. Li, H. Nørgaard, D. M. Warui, S. J. Booker, C. Krebs, J. M. Bollinger, Jr., *J. Am. Chem. Soc.* **2011**, *133*, 6158.

